

Broadband High-Gain Magneto-Electric Dipole Antenna Loaded with T-Slot

Yanyan Wang^{1,2}, Yu Wang³, and Wusheng Ji^{1,2,*}

¹*Institute of Antenna and Microwave Techniques, Tianjin University of Technology and Education, Tianjin 300222, China*

²*School of Electronic Engineering, Tianjin University of Technology and Education, Tianjin 300222, China*

³*Comba Telecom Technology (Guangzhou) Ltd, Guangzhou 510655, Guangdong, China*

ABSTRACT: This paper proposes a magneto-electric dipole antenna with broadband, good directivity, and high gain. By changing the shape of the radiating patch and loading the T-slot to improve the impedance matching ability of the antenna, the bandwidth is effectively expanded. Low cross-polarization and high gain are achieved by using a square metal reflective cavity and a hollow metal cylinder loaded on top of the antenna. Test results show a relative impedance bandwidth ($|S_{11}| < -10$ dB) of 94.4% (1.32 GHz–3.68 GHz) with a maximum gain of 10.7 dBi. The antenna has excellent performance and has applications in wireless communication systems.

1. INTRODUCTION

With the increasing demand of 5G/6G communication system, antenna is developing in the direction of wide bandwidth, high gain, low cross-polarization, and low back-radiation. In 2006, Luk and Wong proposed a magneto-electric dipole antenna for the first time [1], and the relative bandwidth reaches 43.8%, which can meet the requirements of wireless communication systems and has good application value. Broadband antenna can support more communication frequency bands and higher data transmission rate, which better supports the development of wireless communication system.

Magneto-electric dipole antennas have received considerable attention from the academic community due to their excellent performance. To achieve a wider bandwidth, this is usually achieved by changing the shape of the radiating patch, loading parasitic cells, or changing the feed structure. For example, by loading one or more slots in the electrical dipole surface and using an inverted U-shaped feed line [2–4], the impedance bandwidth is effectively increased by more than 15%. A dumb-bell shape patch magneto-electric dipole replaces the traditional rectangular antenna so changing it to a circular structure [5], which makes the equivalent electrical length of the antenna longer and effectively improves the impedance bandwidth of the antenna (93.3%). Using a combination of equivalent magnetic and electrical dipole patches created by a bowtie patch antenna [6], the impedance bandwidth is increased to over 60% by adjusting the spacing or shape of the bowtie patches. In [7, 8], the bandwidth is greatly increased by loading a bowtie slit in the horizontal sheet metal. A new broadband directive antenna consists of a bowtie patch antenna and a dipole [9, 10], where the bandwidth of the antenna is extended to more than 80% by adding a parasitic patch on top of the electric dipole patch.

The impedance bandwidth is boosted by a rectangular electric dipole patch with a rectangular parasitic structure loaded on a curved microstrip feed line [11], resulting in a relative impedance bandwidth of 88% at reflection coefficients less than -15 dB. A relative impedance bandwidth of 75.9% is achieved by exciting the antenna with a trident-type feed line in the case of an asymmetrically structured electric dipole [12]. The use of a low-loss printed ridge-gap waveguide feed network to excite magneto-electric dipoles achieves a wider bandwidth in the high-frequency range from 30 GHz to 50 GHz and above [13–16]. An ultra-wideband impedance matching method is provided by using a parallel double L-shaped differential feed structure [17]: a rectangular cavity instead of a metallic ground plane, achieving an impedance bandwidth of 111.4%. By using a coplanar waveguide with a parallel strapline transition as a feed source [18], a magneto-electric dipole antenna with a wide bandwidth in the millimeter-wave band is obtained, which achieves a bandwidth of 75.76%. The above studies focus on improving the impedance bandwidth of the magnetic dipole; however, the antenna structure is more complex, and the gain is decreased. Therefore, a better balance between bandwidth and gain needs to be considered when broadband magneto-electric dipole antennas are designed.

In order to solve these problems, this paper designs a simple broadband high gain magneto-electric dipole antenna. This antenna introduces a simple defective ground structure on the original vertical rectangular magnetic dipole patch and etches a T-shaped slot on the horizontal patch. These improvements enhance the radiation capability of the electric dipole and expand the bandwidth of the antenna. Meanwhile, the structural design of square metal reflective cavity and hollow metal cylinder significantly improves the antenna gain, which makes the antenna have a more stable radiation direction map, low cross-polarization, as well as low back flap.

* Corresponding author: Wusheng Ji (jiwusheng@tute.edu.cn).

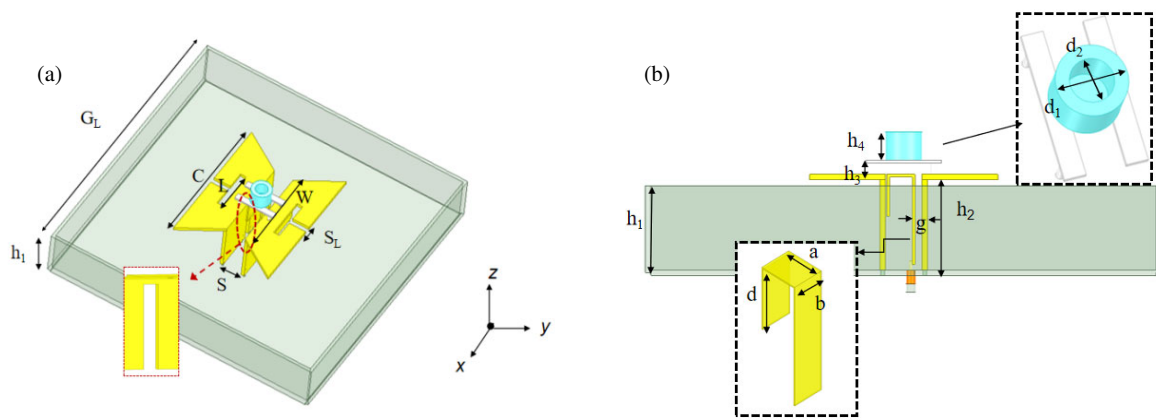


FIGURE 1. Schematic diagram of magneto-dipole antenna structure. (a) 3D view. (b) Side view.

2. ANTENNA DESIGN

2.1. Antenna Structure

The structure of the antenna is shown in Fig. 1. It consists of five main parts: horizontal patches, vertical patches, a Γ -shaped probe feed, a hollow metal cylinder, and a square metal reflective cavity. Horizontal patches are electric dipoles, and vertical patches are magnetic dipoles.

Firstly, the rectangular electric dipole is designed as a trapezoidal structure with the lengths of the upper and lower bottom edges as W and C , respectively. A T-slot of length L and width S_L is etched on the trapezoidal patch. The magnetic dipole patch has a height of h_2 and a width of W and introduces a defect ground structure on the perpendicular magnetic dipole patch [11]. In this way, two electric dipole patches are combined with two perpendicular magnetic dipole patches to form a complementary magneto-electric dipole antenna. Secondly, a coaxial line combined with a Γ -shaped probe feed is used for feeding. The Γ -shaped probe feed is divided into three parts. The first part is connected to the coaxial wire probe to transmit energy to the second part which is placed horizontally; the second part couples the energy above the magneto-electric dipole; and the third part is the end of the Γ -shaped probe feed which is parallel to the first part. Finally, four vertical rectangular metal plates were used around the metal ground plane to form a square metal reflective cavity, and a hollow metal cylinder was loaded on top of the antenna. The four rectangular metal reflectors are the same, with a side length of G_L , a wall height of h_1 , and a thickness of 2 mm; the hollow metal cylinders have a height of h_4 , an outer diameter of d_1 , and an inner diameter of d_2 . The hollow metal cylinder is fixed directly above the antenna with two brackets; the bracket is made of Teflon with a dielectric constant of 2.1, a width of 4 mm, a length of 24 mm, and a

thickness of 1 mm. The hollow metal cylinder is at a height of h_3 from the antenna. The specific dimensions of this antenna are shown in Table 1.

2.2. Antenna Design Theory

A magneto-electric dipole antenna is a special antenna structure that generates radiation through the current distribution on the surface of the antenna element. Fig. 2 demonstrates the current distribution on the surface of the horizontal trapezoidal electric dipole and vertical magnetic dipole during one period of the antenna. From Fig. 2, it can be seen that the surface currents of the electric and magnetic dipoles are the strongest at $t = 0$ as well as $t = T/2$; when $t = T/4$ as well as $t = 3T/4$, the electric and magnetic dipole surface currents become weak. It can be seen that the electric and magnetic dipoles are excited simultaneously in one period [19], realizing the working principle of the magneto-electric dipole antenna.

Similarly, the hollow metal cylinder is excited at the same time as the magneto-electric dipole is excited at $t = 0$ and $t = T/2$. At $t = 0$, an electric field is excited by the magneto-electric dipole, and the energy is coupled to the hollow metal cylinder. Thus, the hollow metal cylinder is excited. When the frequency is close to the intrinsic frequency of the hollow metal cylinder, the inner electro-magnetic field of the antenna will resonate. It is shown that the loading of the hollow metal cylinder enables the effective focusing of energy, which is directed and concentrated along the Z axis. This focusing effect enhances the gain, allowing it to achieve optimal impedance matching and maximum impedance bandwidth.

Figure 3 shows the comparison of the bandwidths and gains of the antenna with and without loading the hollow metal cylinder. In the case of loading a hollow metal cylinder, the gain is increased by 2–3 dBi at high frequency and low frequency. Although the gain at the center frequency is decreased, it also reaches more than 7.2 dBi, and the impedance bandwidth reaches 98.4% ($|S_{11}| < -10$ dB). On the contrary, the bandwidth is only 31% ($|S_{11}| < -10$ dB) without the hollow metal cylinder. The simulation results can verify that the hollow metal cylinder can increase the antenna gain in the operating band and can expand and stabilize the whole passband.

TABLE 1. Antenna geometry.

Parameters	G_L	L	W	a	b	d	g	S_L
Value/mm	180	27	55	9	8	15	2	4
Parameters	h_1	h_2	h_3	h_4	d_1	d_2	S	
Value/mm	31	32	6	10	13	9	15	

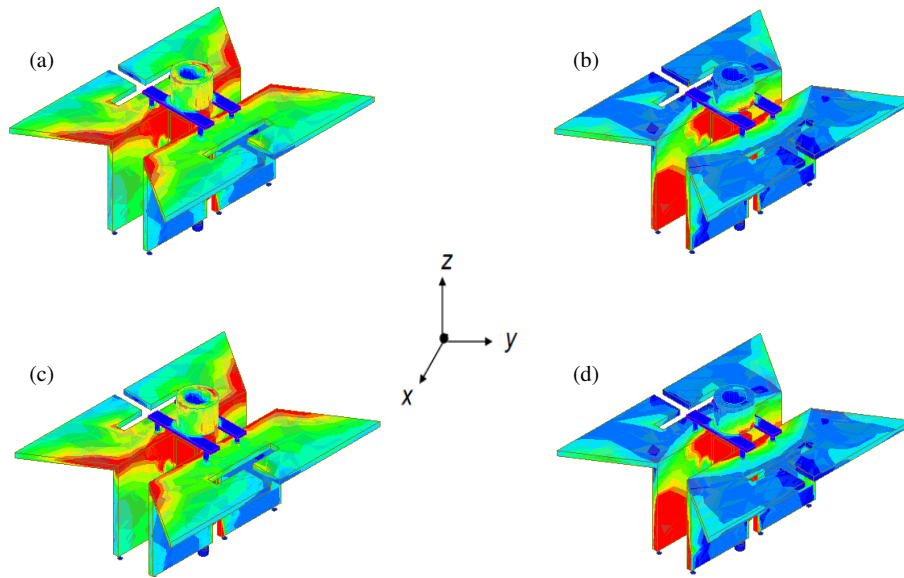


FIGURE 2. Surface current distribution plot. (a) $t = 0$, (b) $t = T/4$, (c) $t = T/2$, (d) $t = 3T/4$.

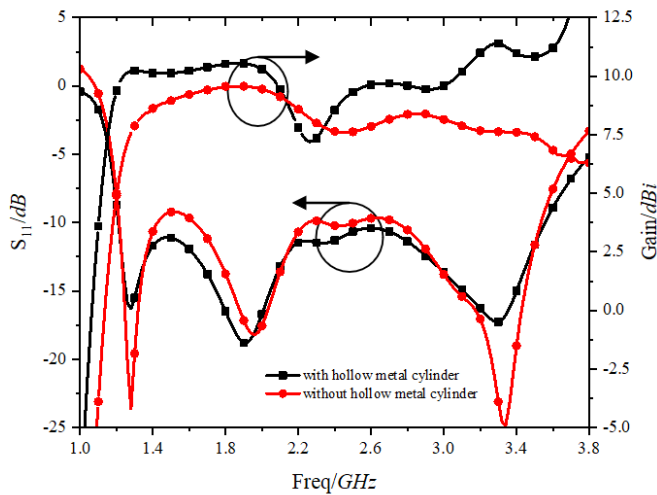


FIGURE 3. Comparison of reflection coefficients and gains of antenna with and without hollow metal cylinders loading.

2.3. Parametric Analysis

The dimensions of each part of the antenna are the main factors that affect the performance of the antenna. In order to explore the effect of each factor on the performance of the designed antenna, the important factors are scanned, and the results of the scanning are shown as follows.

L is the length of the slit parallel to the X axis, and the effect of L on the antenna performance is shown in Fig. 4. It can be seen that when $L = 20$ mm, the low-frequency resonance point moves toward higher frequencies. As the length L increases, the low-frequency resonance point progressively moves to lower frequencies, resulting in a wider bandwidth. However, when L is equal to 30 mm, S_{11} is up to -9 dB at 2.5 GHz, resulting in a narrower impedance bandwidth for the antenna. In order to realize good impedance matching, $L = 27$ mm is chosen.

S_L is the width of the slit parallel to the Y axis, and the effect of S_L on the antenna performance is shown in Fig. 5. It can be found that with the increase of S_L , the resonance point at the high frequency will be shifted upward, and similarly, S_{11} is also worse. When $S_L = 4$ mm, the reflection coefficient is the optimal performance at both the low-frequency and high-frequency resonance points.

h_3 is the vertical height of the hollow metal cylinder from the electric dipole patch, and the effect of h_3 on the antenna performance is shown in Fig. 6. It can be seen that no matter h_3 is greater or less than 6 mm, the resonance point at the high frequency moves to the low frequency, making the bandwidth narrower. At the same time, the gain at the low frequency in the band is slightly increased with the increase of h_3 . When $h_3 = 6$ mm, antenna has the best results in the whole band. Therefore, $h_3 = 6$ mm is chosen to achieve high gain with good impedance matching.

d_1 is the outside diameter of the hollow metal cylinder, and the effect of d_1 on the antenna performance is shown in Fig. 7. The inside diameter remains unchanged when the outer diameter is varied. It can be seen from Fig. 7 that the bandwidth fluctuates as the outside diameter of the hollow metal cylinder increases, and both the high and low frequency resonance points are shifted upward so that most of the frequency points are greater than -10 dB. Meanwhile, the gain decreases with the increase of d_1 . Therefore, $d_1 = 13$ mm is chosen to achieve high gain with good impedance matching.

3. PROCESSING AND DISCUSSION

3.1. Antenna Processing

In order to verify the validity of the antenna design, a prototype antenna is fabricated as shown in Fig. 8. The radiator of the antenna (magneto-electric dipole patch) and the square reflective cavity are made of aluminum alloy of the same thickness (2 mm). The hollow metal cylinders are made of the same alu-

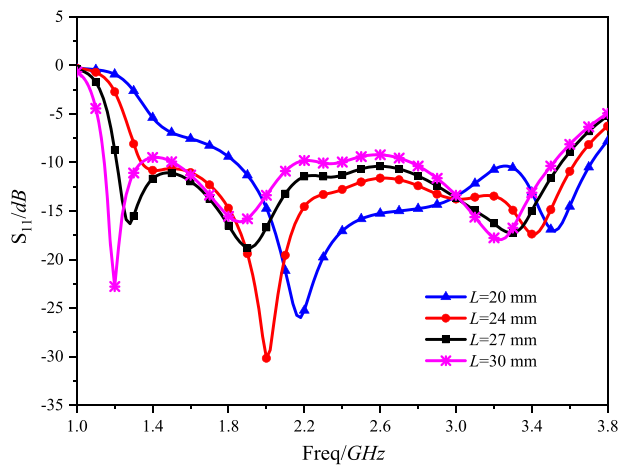


FIGURE 4. Antenna reflection coefficient variation with L .

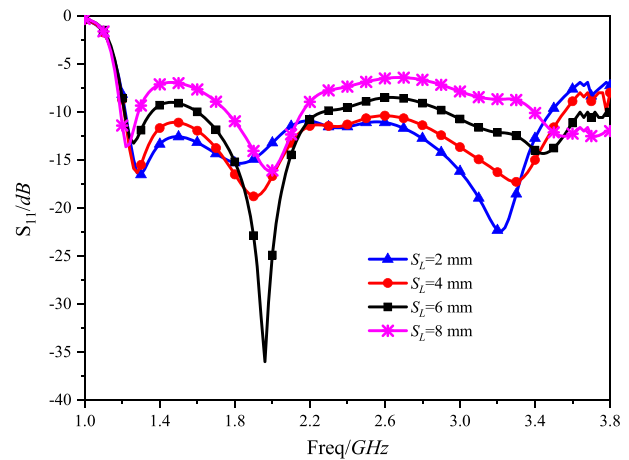


FIGURE 5. Antenna reflection coefficient variation with S_L .

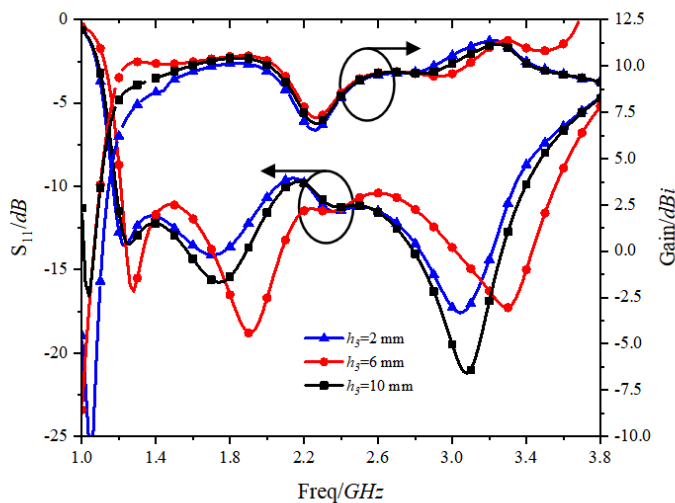


FIGURE 6. Antenna reflection coefficient and gain variation with h_3 .

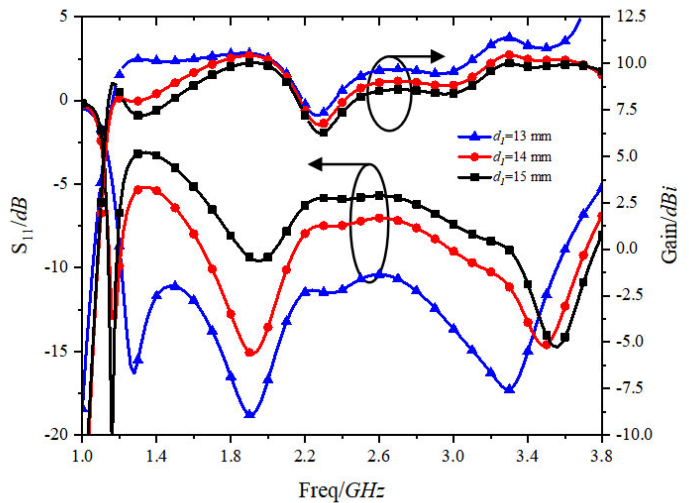


FIGURE 7. Antenna reflection coefficient and gain variation with d_1 .

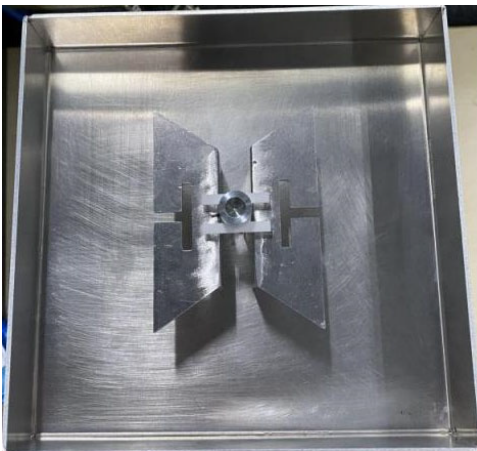


FIGURE 8. Antenna prototype.

minimum alloy. The square reflective cavity is cut and bent from a single aluminum plate to avoid the unevenness that may result from the assembly of four sidewall reflectors. The magnetic dipole patch is secured to the metal ground plane with 8 stain-

less steel screws. The hollow metal cylinder is on top of the antenna and is glued to the Teflon mount. Four holes are made on the surface of the two electric dipole patches, and two cylinders with the diameter of 1 mm are located at the bottom of each support; the cylinders of the supports are inserted into the holes of the electric dipole patches and glued together.

3.2. Bandwidth and Gain

Figure 9 shows the reflection coefficient and gain curves of the magneto-electric dipole antenna simulated and measured in this paper. As shown in Fig. 9, the relative impedance bandwidths ($|S_{11}| < -10$ dB) of the antenna simulated and measured are 98.4% (1.21 GHz–3.55 GHz) and 94.4% (1.32 GHz–3.68 GHz). The simulated and measured gains in the operating band are above 7.2 dBi and 7.9 dBi, and the peak gains are 11.39 dBi and 10.7 dBi for simulation and measurement. The measured relative bandwidth is slightly narrower than the simulated one, and the measured peak gain is 0.3 dBi smaller than the simulated one, and these deviations are within the error tol-

erance. These deviations are related to both the processing accuracy of the antenna and the measurement error.

3.3. Radiation Efficiency

Figure 10 shows the radiation efficiency plot of the antenna. It can be seen that the radiation efficiency of the antenna designed in this paper stays above 0.9 throughout the passband and is relatively stable, showing its excellent energy conver-

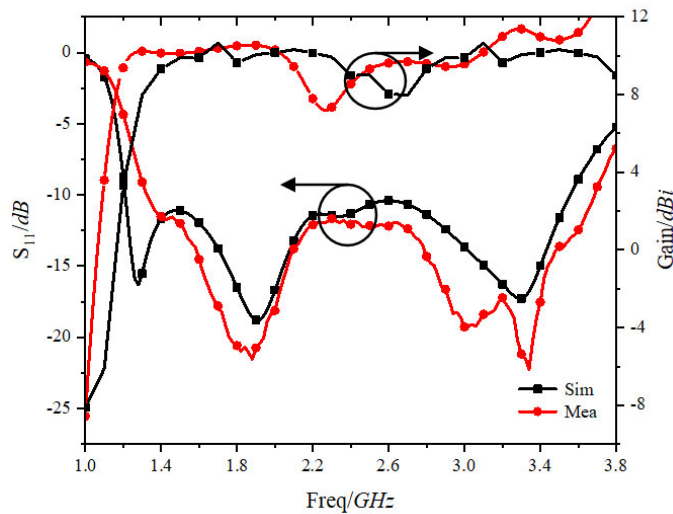


FIGURE 9. Reflection coefficient and gain curves obtained from simulation and measurement.

sion efficiency and ensuring stable performance from low to high frequency.

3.4. Radiation Pattern

Figure 11 shows the simulated and measured radiation direction plots of the proposed antenna at 1.3 GHz, 2.4 GHz, and 3.4 GHz. It is shown in Fig. 11 that the measured antenna radiation direction plots are in high consistency with the simulation results. The *E*-plane and *H*-plane have good sym-

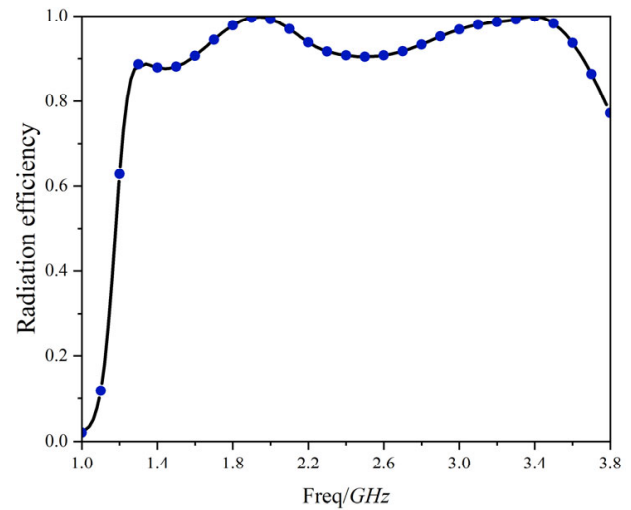
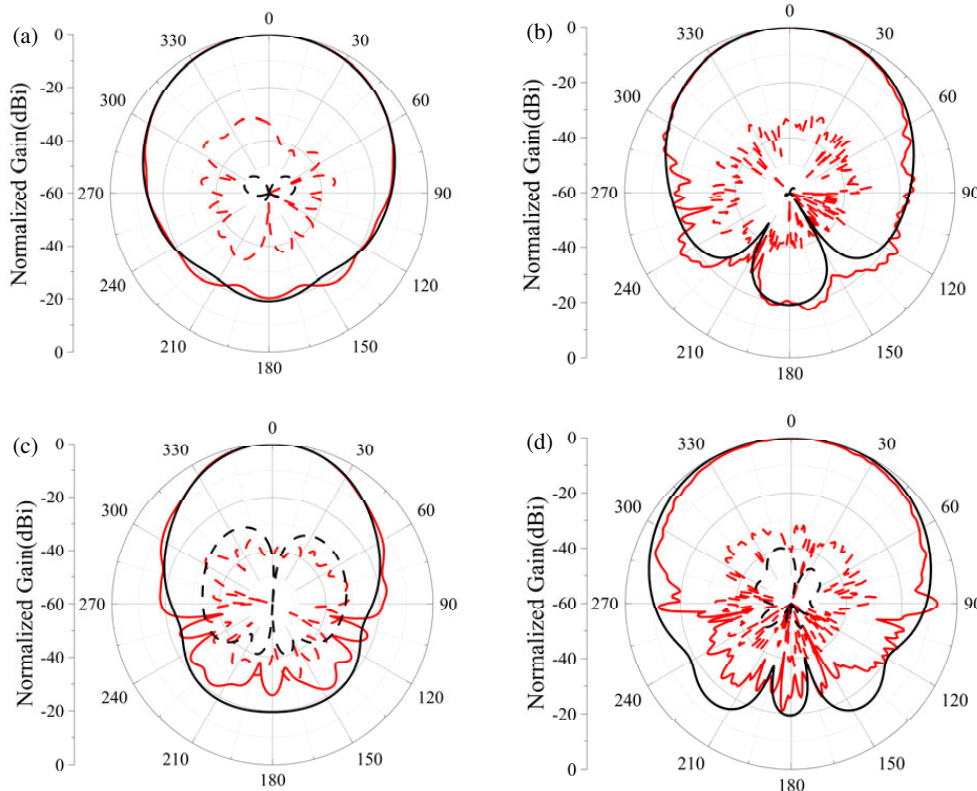


FIGURE 10. Antenna radiation efficiency plot.



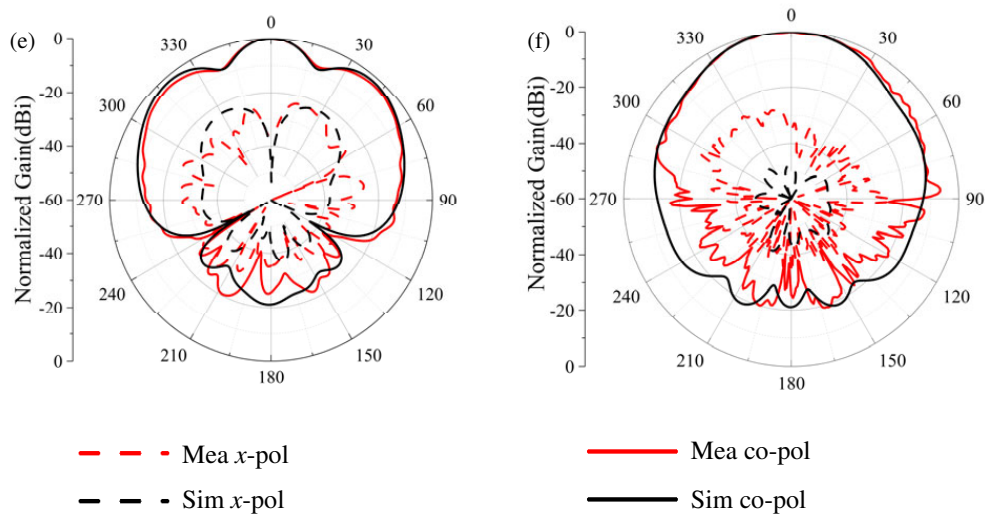


FIGURE 11. Antenna test and simulation radiation pattern plot. (a) 1.3 GHz_E, (b) 1.3 GHz_H, (c) 2.4 GHz_E, (d) 2.4 GHz_H, (e) 3.4 GHz_E, (f) 3.4 GHz_H.

TABLE 2. Comparison of important indicators.

Papers	BW/GHz	Relative Bandwidth/%	Maximum Gain/dBi	Size
[2]	2.45–3.92	46.2	10.19	$1.39\lambda_0 * 1.23\lambda_0 * 0.079\lambda_0$
[5]	1.94–4.72	93.3	8.03	$1.11\lambda_0 * 1.11\lambda_0 * 0.3\lambda_0$
[20]	1.38–3.5	86.9	7.2 ± 1.2	$1.44\lambda_0 * 1.44\lambda_0 * 0.224\lambda_0$
[21]	2.2–5.1	79	9	$1.46\lambda_0 * 1.46\lambda_0 * 0.21\lambda_0$
[22]	1.85–3.65	65	6.28	NA
This work	1.32–3.68	94.4	10.7	$1.44\lambda_0 * 1.44\lambda_0 * 0.384\lambda_0$

* λ_0 is the wavelength at the center frequency in air

metry and no obvious distortion in the whole operating frequency band. The measured and simulated cross-polarizations at 1.3 GHz and 2.4 GHz are less than -30 dB, and the measured cross-polarization at 3.4 GHz is higher than that of the simulation results, but it is still less than -20 dB. The above results show that the antenna presented in this paper exhibits a low cross-polarization and low back-flap unidirectional radiation characteristic.

The main parameters such as relative bandwidth and gain of the present antenna are compared with the 5 references shown in Table 2. From Table 2, it can be seen that paper [2] has a narrower bandwidth than the present antenna although the profile height is smaller than the present antenna, and the relative bandwidth is only 48.2%. The gain of paper [5] is 8.03 dBi, which is lower than the gain of the present antenna, although it has a smaller size and a relative bandwidth of more than 90%. Compared to [20] and [21], where the dimensions are similar, the present antenna not only improves the relative bandwidth by more than 10%, but also improves the maximum gain by 1–2 dBi. Paper [22] merely obtained a relative bandwidth of 65% (1.85–3.65 GHz), which is about 30% lower than the present antenna, and the maximum gain is lower than the present an-

tenna by about 4 dBi. In conclusion, the present antenna exhibits a better performance in terms of bandwidth and gain.

4. CONCLUSION

In this paper, a broadband high-gain magneto-electric dipole antenna is proposed, in which the bandwidth of the antenna is improved by changing the shape of the magneto-electric dipole and introducing a T-slot, and the gain in the frequency band is sharply increased by introducing a square metal reflective cavity and a hollow metal cylinder. The test results of the antenna prototype show that the results of bandwidth and gain are basically consistent with the simulation data, and the impedance bandwidth is about 94.4% when $|S_{11}| < -10$ dB; the gains are all kept above 7.9 dBi, and the maximum gain in the band reaches 10.7 dBi. The antenna obtains symmetric and stable radiation direction diagrams with low cross-polarization in the operating band, which proves the validity of the antenna design. The magneto-electric dipole antenna has excellent performances such as broadband, high gain, low cross-polarization, and low back-flap, which is promising for application.

ACKNOWLEDGEMENT

This work is supported by Tianjin Key Projects of Research and Development and Science and Technology Support in 2020 (20YFZCGX00700), and Tianjin Enterprise Science and Technology Commissioner Project in 2022 (22YDTPJC00330).

REFERENCES

- [1] Luk, K.-M. and H. Wong, "A new wideband unidirectional antenna element," *International Journal of Microwave and Optical Technology*, Vol. 1, No. 1, 35–44, 2006.
- [2] Liu, W., T. Wang, D. Gao, Y. Liu, and X. Zhang, "Low-profile broadband magnetolectric dipole antenna with dual-complementary source," *IEEE Antennas and Wireless Propagation Letters*, Vol. 19, No. 12, 2447–2451, Dec. 2020.
- [3] Li, M. and K.-M. Luk, "A differential-fed magneto-electric dipole antenna for UWB applications," *IEEE Transactions on Antennas and Propagation*, Vol. 61, No. 1, 92–99, Jan. 2013.
- [4] Zhang, G., L. Ge, J. Wang, and J. Yang, "Design of a 3-D integrated wideband filtering magneto-electric dipole antenna," *IEEE Access*, Vol. 7, 4735–4740, 2018.
- [5] Ling, M., Y. Du, and J. Li, "A wideband high gain dumbbells-shaped magnetolectric dipole antenna," in *2022 IEEE MTT-S International Microwave Workshop Series on Advanced Materials and Processes for RF and THz Applications (IMWS-AMP)*, 1–3, Guangzhou, China, 2022.
- [6] Wong, H., K.-M. Mak, and K.-M. Luk, "Wideband shorted bowtie patch antenna with electric dipole," *IEEE Transactions on Antennas and Propagation*, Vol. 56, No. 7, 2098–2101, Jul. 2008.
- [7] Ge, L. and K. M. Luk, "A wideband magneto-electric dipole antenna," *IEEE Transactions on Antennas and Propagation*, Vol. 60, No. 11, 4987–4991, Nov. 2012.
- [8] Ding, C. and K.-M. Luk, "Low-profile magneto-electric dipole antenna," *IEEE Antennas and Wireless Propagation Letters*, Vol. 15, 1642–1644, 2016.
- [9] Mao, B. and G. Hua, "A novel wideband unidirectional antenna composed of a shorted bowtie patch antenna and a printed dipole," in *2020 9th Asia-Pacific Conference on Antennas and Propagation (APCAP)*, 1–2, Xiamen, China, 2020.
- [10] Fan, F.-F., Q.-L. Chen, Y.-X. Xu, X.-F. Zhao, J.-C. Feng, and Z.-H. Yan, "A wideband compact printed dipole antenna array with SICL feeding network for 5G application," *IEEE Antennas and Wireless Propagation Letters*, Vol. 22, No. 2, 283–287, Feb. 2023.
- [11] Chang, L., J.-Q. Zhang, L.-L. Chen, and B.-M. Li, "Bandwidth-enhanced cavity-backed magneto-electric dipole antenna," *IEEE Access*, Vol. 6, 62 482–62 489, 2018.
- [12] Wang, M., Y. Mo, W. Luo, H. Yang, and Z. Chen, "Design and measurement of a novel metal-only wideband magneto-electric dipole antenna using asymmetrical structure," *Electronics Letters*, Vol. 57, No. 22, 827–829, 2021.
- [13] Ali, M. M. M., I. Afifi, and A.-R. Sebak, "A dual-polarized magneto-electric dipole antenna based on printed ridge gap waveguide technology," *IEEE Transactions on Antennas and Propagation*, Vol. 68, No. 11, 7589–7594, Nov. 2020.
- [14] Allam, A. M. M. A., A. O. Mahmoud, D. E. Fawzy, and M. Askar, "Ultra wide-band PRGW based magneto-electric dipole antenna," in *2021 15th European Conference on Antennas and Propagation (EuCAP)*, 1–5, Dusseldorf, Germany, 2021.
- [15] Mousavirazi, Z., V. Rafiei, M. M. M. Ali, and T. A. Denidni, "Wideband and low-loss magneto-electric dipole antenna fed by printed ridge-gap waveguide technology," in *2021 IEEE 19th International Symposium on Antenna Technology and Applied Electromagnetics (ANTEM)*, 1–2, Winnipeg, MB, Canada, 2021.
- [16] Ali, M. M. M., M. Al-Hasan, I. B. Mabrouk, and T. A. Denidni, "Ultra-wideband hybrid magneto-electric dielectric-resonator dipole antenna fed by a printed RGW for millimeter-wave applications," *IEEE Access*, Vol. 10, 2028–2036, 2021.
- [17] Li, M. and K.-M. Luk, "A differential-fed magneto-electric dipole antenna for ultra-wideband applications," in *2011 IEEE International Symposium on Antennas and Propagation (AP-SURSI)*, 1482–1485, Spokane, WA, USA, 2011.
- [18] Singh, A. and C. E. Saavedra, "Low-profile CPW-PS-fed magnetolectric antenna," *IEEE Antennas and Wireless Propagation Letters*, Vol. 20, No. 12, 2471–2475, 2021.
- [19] Ge, L. and K.-M. Luk, "Linearly polarized and dual-polarized magneto-electric dipole antennas with reconfigurable beamwidth in the H -plane," *IEEE Transactions on Antennas and Propagation*, Vol. 64, No. 2, 423–431, 2015.
- [20] Zeng, J. and K.-M. Luk, "A simple wideband magnetolectric dipole antenna with a defected ground structure," *IEEE Antennas and Wireless Propagation Letters*, Vol. 17, No. 8, 1497–1500, Aug. 2018.
- [21] Tang, G., Z. Wei, H. Li, X. Du, J. Ren, and Y. Yin, "Design of wideband filtering magnetolectric dipole antenna with a flat gain utilizing U-shaped slot," in *2020 International Conference on Microwave and Millimeter Wave Technology (ICMMT)*, 1–3, Shanghai, China, 2020.
- [22] Prasad, V. and M. Sreenivasan, "Wideband widebeam dual polarized magneto electric dipole antenna," in *2022 IEEE Microwave, Antennas, and Propagation Conference (MAPCON)*, 621–624, Bangalore, India, 2022.